LETTERS
PUBLISHED ONLINE: 4 JANUARY 2016 | DOI: 10.1038/NCLIMATE2913
nature climate change

Regional estimates of the transient climate response to cumulative CO_2 emissions

Martin Leduc[1,2]*, H. Damon Matthews[1]* and Ramón de Elía[2]

The Transient Climate Response to cumulative carbon Emissions (TCRE) measures the response of global temperatures to cumulative CO_2 emissions[1–4]. Although the TCRE is a global quantity, climate impacts manifest predominantly in response to local climate changes. Here we quantify the link between CO_2 emissions and regional temperature change, showing that regional temperatures also respond approximately linearly to cumulative CO_2 emissions. Using an ensemble of twelve Earth system models, we present a novel application of pattern scaling[5,6] to define the regional pattern of temperature change per emission of CO_2. Ensemble mean regional TCRE values range from less than 1 °C per TtC for some ocean regions, to more than 5 °C per TtC in the Arctic, with a pattern of higher values over land and at high northern latitudes. We find also that high-latitude ocean regions deviate more strongly from linearity as compared to land and lower-latitude oceans. This suggests that ice-albedo and ocean circulation feedbacks are important contributors to the overall negative deviation from linearity of the global temperature response to high levels of cumulative emissions. The strong linearity of the regional climate response over most land regions provides a robust way to quantitatively link anthropogenic CO_2 emissions to local-scale climate impacts.

The TCRE is defined as the ratio of global surface air temperature change to cumulative CO_2 emissions, accounting for both physical climate processes, as well as the dynamics of land and ocean carbon sinks[1,3,4]. The TCRE has been shown to be approximately constant in time and independent of the emission pathway, reflecting a near-linear relationship between cumulative CO_2 emissions and global temperature change[7–9] (Supplementary Fig. 1a). Furthermore, the spatial pattern of temperature change per degree of global warming (Supplementary Fig. 1b) has also been shown to remain approximately constant with increasing global mean temperature increases[5,6,10,11]. Therefore, there is considerable potential and utility in assessing the regional temperature response to cumulative CO_2 emissions, combining the widely used pattern-scaling approach with the methodology used to calculate the global TCRE.

Here, we quantify the spatial pattern of temperature change per emission of CO_2 (Fig. 1a; see Methods). The spatial pattern of regional TCRE (hereafter referred to as RTCRE) values is characterized by high contrasts between land and ocean, with values generally smaller than 1.5 °C per TtC over low- and mid-latitude ocean regions, and values over land ranging from 1.5 to 4 °C per TtC. The highest RTCRE values occur over the Arctic region (>4.5 °C per TtC), with a maximum value near the Barents and Kara seas (>5.5 °C per TtC). Average land (Fig. 1b) and ocean (Fig. 1c) temperatures both show a near-linear response to cumulative CO_2 emissions; we estimate a land-only TCRE of 2.2 ± 0.5 °C per TtC, compared to 1.4 ± 0.3 °C for the ocean-only TCRE. For this ensemble of 12 CMIP5 models, the global TCRE is 1.7 ± 0.4 °C per TtC (see Methods and Supplementary Fig. 1a).

The near-linearity seen in Fig. 1b,c also holds for smaller regions. Figure 2 shows the time series of the regional temperature response to cumulative CO_2 emissions over the 21 Giorgi land regions[12] (see Supplementary Fig. 2 for the location of these regions). These regional responses are generally highly linear, and most also show a relatively small inter-model range compared to the mean response. The clearest examples are the regions of Central America (1.8 ± 0.4 °C per TtC; panel d), Eastern Africa (1.9 ± 0.4 °C per TtC; panel m) and Southeast Asia (1.5 ± 0.3 °C per TtC; panel p). A few regions, however, show a relatively large spread across model responses, notably Alaska (3.6 ± 1.4 °C per TtC; panel h), Greenland (3.1 ± 0.9 °C per TtC; panel i) and North Asia (3.1 ± 0.9 °C per TtC; panel u).

The spatial pattern of the inter-model spread (IMS) of RTCRE values (shown in Fig. 3a as one standard deviation of the ensemble) shows generally higher uncertainty at high latitudes, compared to mid- and low-latitude regions. The largest uncertainty in the RTCRE pattern occurs over the Arctic Ocean ($>\pm 1.8$ °C per TtC). The uncertainty is also large over Hudson Bay, Alaska, Greenland Sea, the Sea of Okhotsk ($>\pm 1.4$ °C per TtC) and the Southern Ocean ($>\pm 0.8$ °C per TtC). Most land areas and mid-latitude ocean regions are therefore associated with a small inter-model spread, and also carry an RTCRE estimate that is greater than three times the uncertainty range (see Supplementary Fig. 3).

In general, the inter-model uncertainty values shown here include a contribution from natural variability, as well as from model differences in climate and carbon cycle sensitivities to emissions. With the exception of a few high-latitude regions with higher natural variability[13], the natural variability generally explains a small fraction of the inter-model spread (Fig. 3b; see Methods). Therefore, the primary contributor to the RTCRE spread shown here comes from model differences in climate and carbon cycle sensitivities. However, it is also interesting to consider whether these model differences manifest as a result of differences in the global TCRE value among models, or model differences in the regional patterns of temperature change associated with a given global TCRE value (see Methods). As shown in Fig. 3c, the pattern-based uncertainty among models dominates at high latitudes and over most land regions, whereas the RTCRE uncertainty over mid- and low-latitude oceans is almost entirely explained by model differences in the global temperature response to cumulative emissions.

As in the case of the global TCRE, the regional temperature changes shown here are apparently linearly related to cumulative CO_2 emissions. At the global scale, this linearity has been argued

[1]Concordia University, Department of Geography, Planning and Environment, 1455 de Maisonneuve Blvd. W, Montreal, Quebec H3C 1MB, Canada. [2]Ouranos, 550 Sherbrooke West, West Tower, 19th floor, Montreal, Quebec H3A 1B9, Canada. *e-mail: leduc.martin@ouranos.ca; damon.matthews@concordia.ca

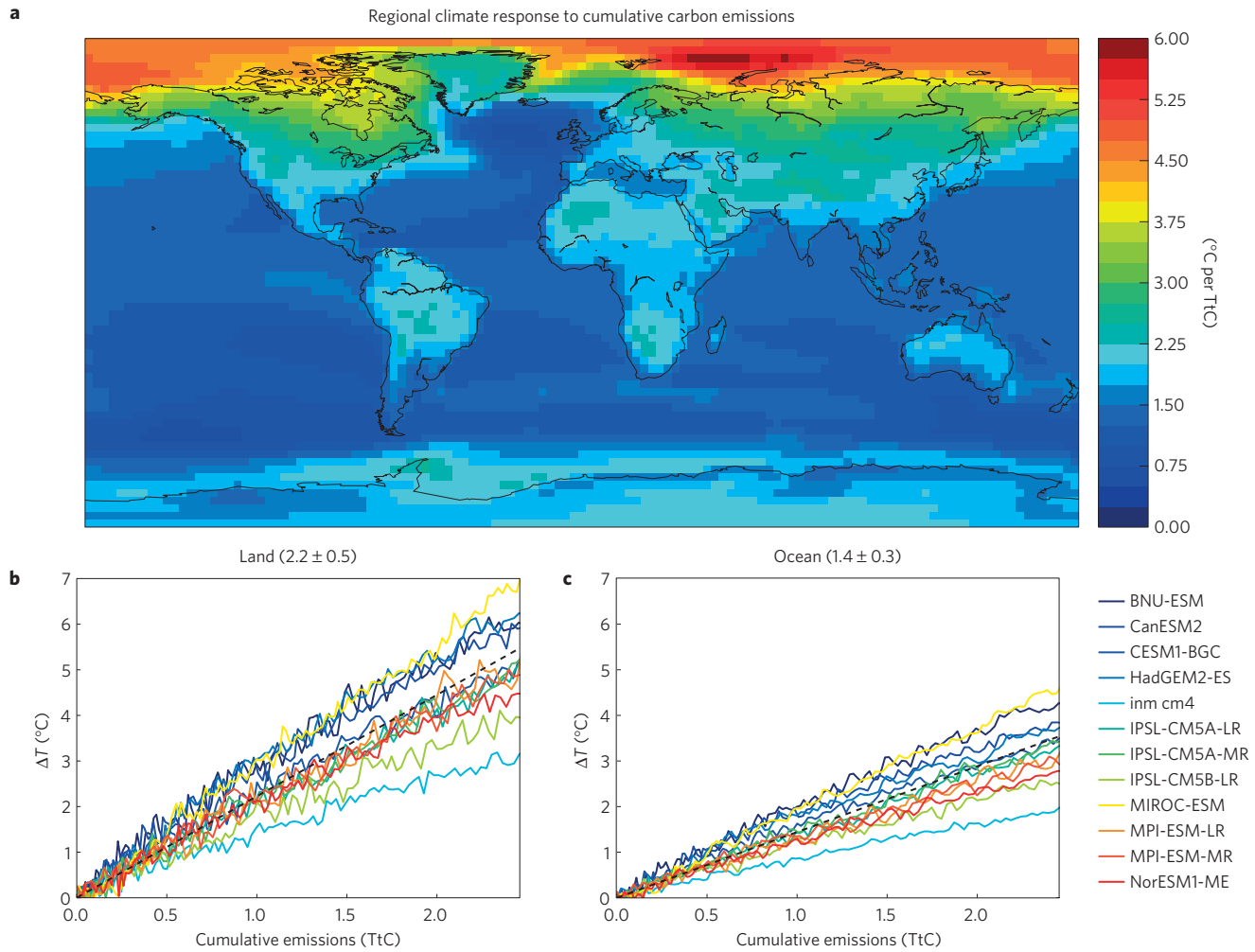

Figure 1 | The pattern of temperature change per CO_2 emission. a, Regional TCRE (RTCRE) ensemble mean values calculated at the time of CO_2 doubling using 20-year average windows. **b**,**c**, Overall land (**b**) and ocean temperature (**c**) responses to cumulative CO_2 emissions for each model and for the ensemble mean (dashed line). For this ensemble of 12 CMIP5 models, the mean responses are 2.2 °C per TtC over land and 1.4 °C per TtC for the ocean, with a uncertainty ranges given as 1 standard deviation.

to occur as a result of the compensation of ocean carbon and heat uptake[14], as well as the balance over time of opposing nonlinear changes in the strength of carbon sinks and the radiative forcing from CO_2 (ref. 1). Previous analyses of the global TCRE have also identified a departure from linearity at high levels of cumulative emissions[1,3,4,9], and have argued that this can be explained by the diminishing effectiveness of CO_2 radiative forcing becoming more prominent than the effect of weakening carbon sinks (and hence increasing airborne fraction of CO_2 emissions) at higher atmospheric CO_2 levels[1,9,14]. However, close examination of Fig. 2 suggests that there are also differences in the robustness of this linear assumption among regions. This suggests in turn that regionally specific climate feedbacks affect the linearity of the RTCRE, and may also be important contributors to the negative deviation from linearity evident in the global TCRE.

To quantify the relative linearity of regional temperature responses to cumulative emissions, we calculated the sum of squared errors (SSE) for linear and quadratic fits to the temperature-cumulative emissions relationship (see Methods). The ratio of these two SSE values (defined here as $Q = \mathrm{SSE}_{\mathrm{linear}}/\mathrm{SSE}_{\mathrm{quadratic}}$) represents the amount of variability that is unexplained by the linear relative to the quadratic fit, and therefore represents a measure of the quality of the linearity assumption for each time series (where a ratio close to unity indicates that the quadratic model does not improve the fit to the data, and we should therefore accept the simpler linear fit). However, it is also the case that the amount of natural variability in a given time series affects our ability to detect a weak deviation from linearity. We therefore also calculated the signal-to-noise ratio (S; see Methods) to represent the effect of natural variability on the linearity of the regional temperature responses to cumulative emissions.

The spatial distributions of Q (Fig. 4a) and S (Fig. 4b) values are therefore together able to identify those regions that deviate the most from a linear temperature response to emissions. Maximum Q values ($Q = 1.3$) occur in the Arctic region (extending over the Barents and Kara seas), indicating a region of relatively weak linearity. Ocean regions surrounding Southeast Asia generally show intermediate Q values ($Q = 1.15$), and strongly linear regions (Q near 1) occur over land regions in general, as well as over a large portions of the oceans. By comparing the patterns in Fig. 4a,b, it is evident that there is a strong correlation between Q and S values over most of the map, with the notable exceptions of high-latitude ocean points in the North Atlantic, the Arctic—and to a lesser extent also in the Southern Ocean. These regions of high Q and low S values are therefore the regions where the temperature response to emissions most clearly deviates from a linear relationship.

The effect of this larger negative deviation from linearity over high-latitude ocean regions can been seen clearly in Fig. 4c, which

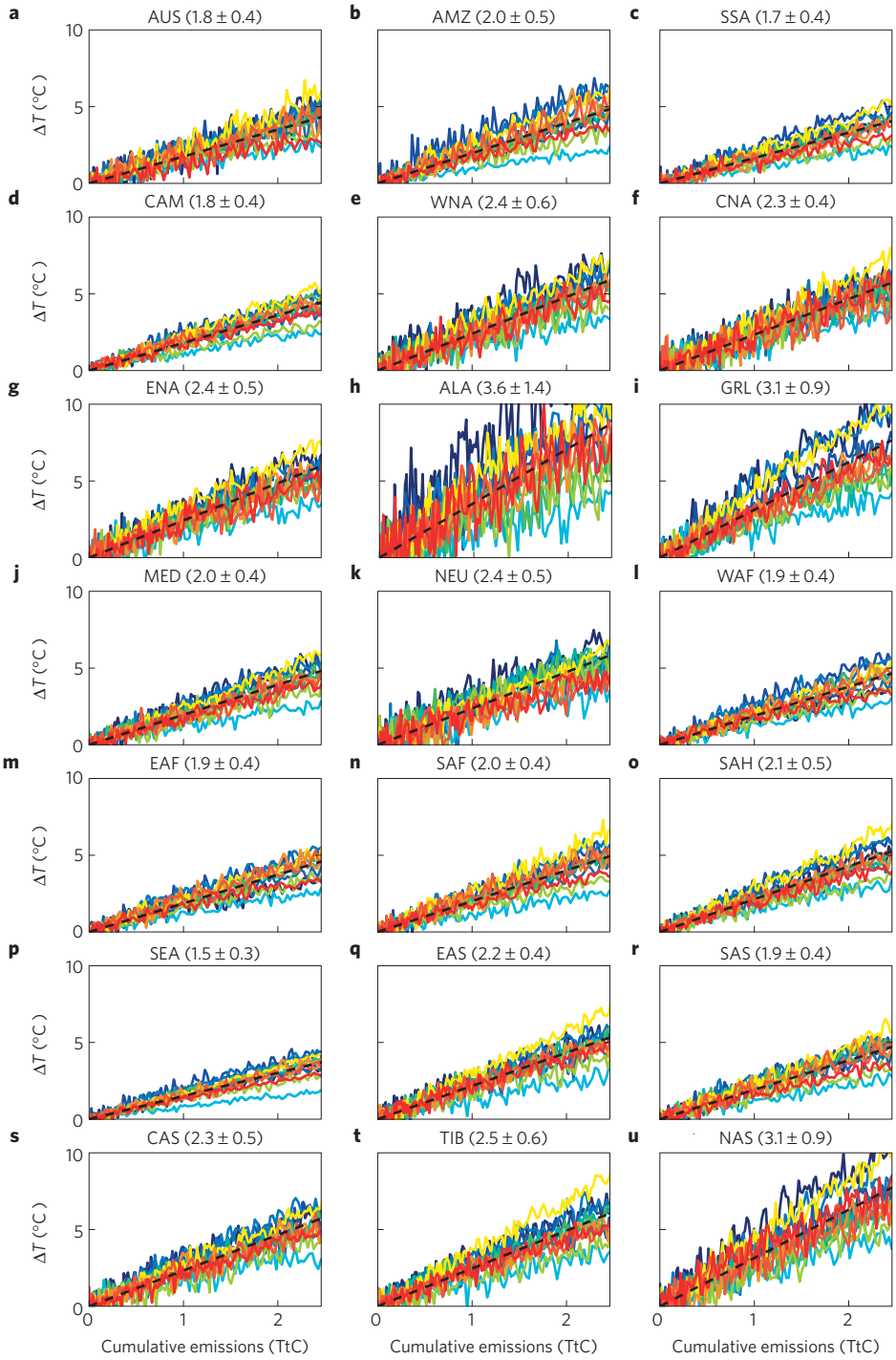

Figure 2 | RTCRE estimates and time series of the regional temperature response to cumulative emissions calculated over 21 land regions. Region definitions are taken from ref. 12 as shown in Supplementary Fig. 2: Australia (AUS), Amazon Basin (AMZ), Southern South America (SSA), Central America (CAM), Western North America (WNA), Central North America (CNA), Eastern North America (ENA), Alaska (ALA), Greenland (GRL), Mediterranean Basin (MED), Northern Europe (NEU), Western Africa (WAF), Eastern Africa (EAF), Southern Africa (SAF), Sahara (SAH), Southeast Asia (SEA), East Asia (EAS), South Asia (SAS), Central Asia (CAS), Tibet (TIB) and North Asia (NAS).

plots the Q and S values for each grid point (coloured by latitude from the North (red) to South (blue) poles). From this plot, we can see first that the vast majority of locations are highly linear, with Q values less than 1.1 over 86% of all grid points and over 97% of land grid points (characterized by the 'January ITCZ' point marked on the plot). Second, we can see that there is also a general pattern of increasing Q with increasing S, as represented by the cloud of points sloping upwards towards the 'Indonesia' point; this relationship therefore reflects a globally consistent negative deviation from linearity, which becomes easier to detect (increasing Q) with increasing S values. Third, there is a distinct cloud of mostly high-latitude locations (including the highlighted 'Barents Sea' point) which deviates from the global pattern by exhibiting relatively high Q values despite their small S values. These grid points are primarily ocean cells (see Supplementary Fig. 4, as well as Q and S values calculated for each individual model in Supplementary

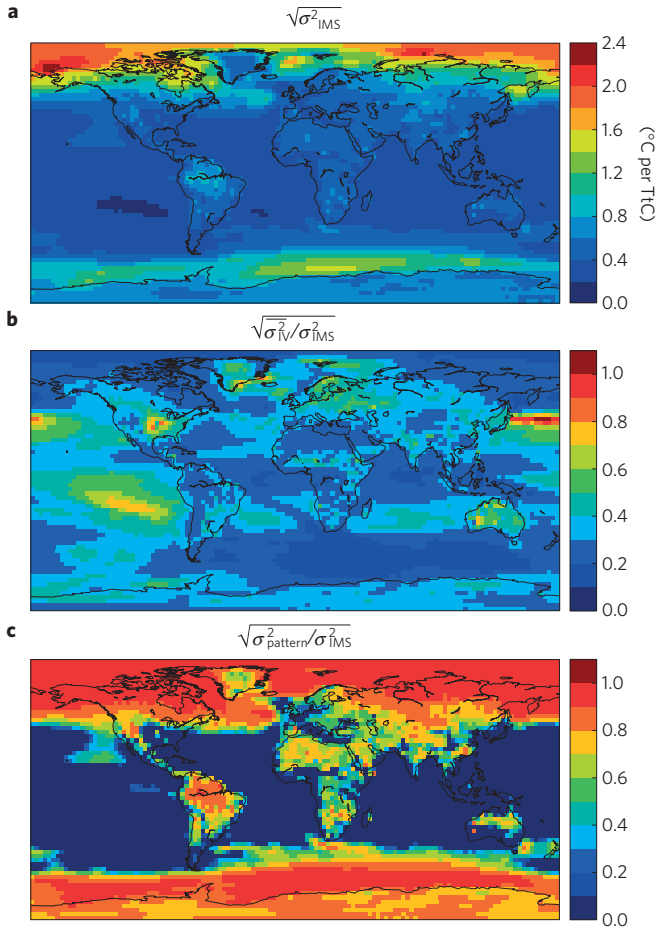

Figure 3 | Characterization of the inter-model spread of RTCRE values. **a**, Intermodel spread of RTCRE values (calculated as one standard deviation), showing considerably higher uncertainty in the high-latitude climate response to emissions. **b**, Plot indicating that the contribution of natural variability to this spread is generally small. **c**, Plot indicating the contribution of uncertainty from model differences in the pattern of temperature change (for a given global TCRE value) is large at high latitudes and over many land areas (suggesting a dominant contribution from pattern-scaling uncertainty in these locations), and is small over tropical/mid-latitude oceans (suggesting a dominant contribution from variation in the global TCRE response among models).

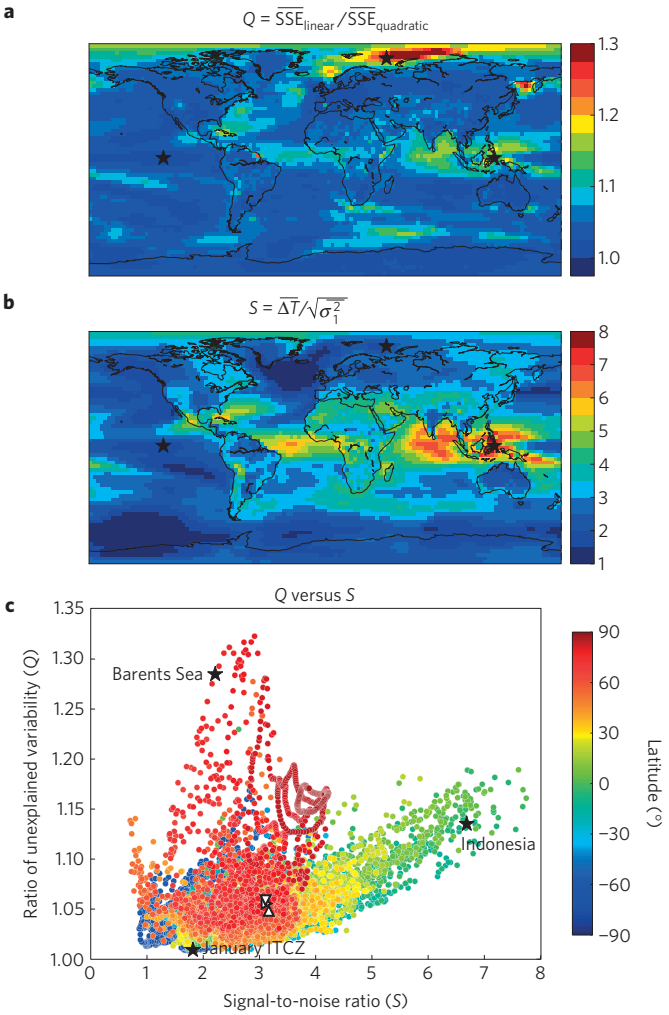

Figure 4 | Characterization of the relative linearity of regional temperature responses to cumulative emissions. a, The ratio of sum of squared errors (SSE) for the linear fit (SSE_{linear}) over the quadratic ($SSE_{quadratic}$) fits (Q) as a measure of the quality of the linear assumption at each grid point, where values closer to unity reflect stronger linearity. **b**, Signal-to-noise ratio (S), a factor affecting how well Q is able to detect deviations from linearity. **c**, Combination of Q and S values at each grid point shows which locations deviate most strongly from the linearity assumption. Here, each circle represents one grid point, coloured by latitude. Three representative grid points are denoted with stars, and the spatially averaged land, ocean and global Q/S values are labelled as △, ▽ and ▷.

Figs 6–10) that are affected strongly by local nonlinear climate feedbacks such that the local warming per unit CO_2 emission decreases with time and increasing cumulative emissions.

As can be seen from the spatially averaged land, ocean and global Q and S values marked on Fig. 4, these areas of locally decreased linearity are sufficient to decrease the linearity of both the ocean and global TCRE, relative to the land-only average. This regional analysis therefore provides some new insight as to why the global TCRE deviates from linearity at high levels of cumulative emissions. First, the global correlation between Q and S is consistent with the effect of the radiative saturation of CO_2 forcing at high CO_2 concentrations, which has been evoked previously to explain the curvature in the global TCRE relationship[1,3,4]. However, our analysis demonstrates that regional processes and feedbacks make an additional contribution to this global trend. Given the high-latitude location of the regions characterized by weaker linearity, there are two possible mechanistic explanations for this negative deviation from linearity. First, a weakening of ice-albedo feedbacks, as snow and ice cover decreases with increasing temperature change, would lead to less local warming with increasing cumulative emissions. Second, a weakening of the ocean's meridional overturning circulation over time would also slow the rate of warming in this region. Recent research has highlighted the important role of these high-latitude feedbacks as drivers of regional climate changes[15–18]. Our results further suggest that the changing strength of these regional feedbacks over time also contribute to the negative deviation of the global TCRE from linearity at high cumulative emissions.

The regional patterns of RTCRE values that we have presented here demonstrate that pattern-scaling approaches[6,10] can be usefully extended to calculate regional temperature changes as a function of cumulative CO_2 emissions. Furthermore, we have shown that most locations show a highly linear temperature response to emissions, and that this linear assumption is particularly robust over land regions. Although we have excluded non-CO_2 gases from our analysis, the similarity that had been found previously between patterns of greenhouse gas and aerosol-induced temperature

changes[19] suggests the potential to apply pattern scaling to calculate the regional climate response to a broader range of emissions. There may also be potential to apply this approach to precipitation, given that annual mean precipitation patterns have been shown to scale well with global temperature[6,20], and that there is also some evidence of a proportional relationship between global average precipitation and cumulative CO_2 emissions[8].

In the most recent IPCC Assessment report, the global TCRE was defined to be well approximated by a constant value (likely to be within the range of 0.8–2.5 °C per TtC) under conditions of increasing global temperatures, and up to total emissions of 2000 GtC (ref. 4). On the basis of our analysis here, it seems that the regional temperature responses to cumulative emissions can also be well approximated by a set of near-constant RTCRE values. Our findings therefore represent a clear quantitative link between CO_2 emissions and local climate warming, which provides a novel mechanism by which to attribute local-scale climate impacts directly to global CO_2 emissions.

Methods

Methods and any associated references are available in the online version of the paper.

Received 22 August 2015; accepted 7 December 2015; published online 4 January 2016

References

1. Matthews, H. D., Gillett, N. P., Stott, P. A. & Zickfeld, K. The proportionality of global warming to cumulative carbon emissions. *Nature* **459,** 829–832 (2009).
2. Allen, M. R. *et al*. Warming caused by cumulative carbon emissions towards the trillionth tonne. *Nature* **458,** 1163–1166 (2009).
3. Gillett, N. P., Arora, V. K., Matthews, H. D. & Allen, M. R. Constraining the ratio of global warming to cumulative CO_2 emissions using CMIP5 simulations. *J. Clim.* **26,** 6844–6858 (2013).
4. Collins, M. *et al*. in *Climate Change 2013: The Physical Science Basis* (eds Stocker, T. F. *et al*.) 1029–1136 (IPCC, Cambridge Univ. Press, 2013).
5. Santer, B., Wigley, T., Schlesinger, M. & Mitchell, J. *Developing Climate Scenarios from Equilibrium GCM Results* 47 (Hamburg, Germany, 1990).
6. Tebaldi, C. & Arblaster, J. M. Pattern scaling: its strengths and limitations, and an update on the latest model simulations. *Climatic Change* **122,** 459–471 (2014).
7. Matthews, H. D., Solomon, S. & Pierrehumbert, R. Cumulative carbon as a policy framework for achieving climate stabilization. *Phil. Trans. R. Soc. A* **370,** 4365–4379 (2012).
8. Zickfeld, K., Arora, V. K. & Gillett, N. P. Is the climate response to CO_2 emissions path dependent? *Geophys. Res. Lett.* **39,** L05703 (2012).
9. Leduc, M., Matthews, H. D. & de Elía, R. Quantifying the limits of a linear temperature response to cumulative CO_2 emissions. *J. Clim.* **28,** 9955–9968 (2015).
10. Mitchell, T. D. Pattern scaling: an examination of the accuracy of the technique for describing future climates. *Climatic Change* **60,** 217–242 (2003).
11. Solomon, S. *et al*. *Climate Stabilization Targets: Emissions, Concentrations, and Impacts over Decades to Millennia* (National Academies, 2011).
12. Giorgi, F. & Francisco, R. Uncertainties in regional climate change prediction: a regional analysis of ensemble simulations with the HADCM2 coupled AOGCM. *Clim. Dynam.* **16,** 169–182 (2000).
13. Deser, C., Phillips, A., Bourdette, V. & Teng, H. Uncertainty in climate change projections: the role of internal variability. *Clim. Dynam.* **38,** 527–546 (2012).
14. Goodwin, P., Williams, R. G. & Ridgwell, A. Sensitivity of climate to cumulative carbon emissions due to compensation of ocean heat and carbon uptake. *Nature Geosci.* **8,** 29–34 (2015).
15. Good, P. *et al*. Nonlinear regional warming with increasing CO_2 concentrations. *Nature Clim. Change* **5,** 138–142 (2015).
16. Jonko, A. K., Shell, K. M., Sanderson, B. M. & Danabasoglu, G. Climate feedbacks in CCSM3 under changing CO_2 forcing. Part II: variation of climate feedbacks and sensitivity with forcing. *J. Clim.* **26,** 2784–2795 (2013).
17. Colman, R. & McAvaney, B. Climate feedbacks under a very broad range of forcing. *Geophys. Res. Lett.* **36,** l01702 (2009).
18. Hansen, J. *et al*. Earth's energy imbalance: confirmation and implications. *Science* **308,** 1431–1435 (2005).
19. Boer, G. & Yu, B. Climate sensitivity and climate state. *Clim. Dynam.* **21,** 167–176 (2003).
20. Ruosteenoja, K., Tuomenvirta, H. & Jylhä, K. GCM-based regional temperature and precipitation change estimates for Europe under four SRES scenarios applying a super-ensemble pattern-scaling method. *Climatic Change* **81,** 193–208 (2007).

Acknowledgements

The authors recognize the financial contribution of the Concordia Institute for Water, Energy and Sustainable Systems (NSERC CREATE grant), HDM's NSERC Discovery Grant and Concordia University Research Chair research grant, the Ouranos Consortium, the 'Fonds de recherche en sciences du climat d'Ouranos' (FRSCO) programme, the Office of the Vice-President, Research and Graduate Studies at Concordia University and the Global Environmental and Climate Change Centre (GEC3). The authors also wish to thank N. Gillett and B. G. St-Denis for their technical help and P. Goodwin and the Concordia Climate Science, Impacts and Mitigation Studies (C2SIMS) group for insightful discussions. We finally acknowledge the World Climate Research Programme's Working Group on Coupled Modelling, which is responsible for CMIP, and we thank the climate modelling groups for producing and making available their model output. For CMIP, the US Department of Energy's Program for Climate Model Diagnosis and Inter-comparison provides coordinating support and led development of software infrastructure in partnership with the Global Organization for Earth System Science Portals.

Author contributions

M.L. and H.D.M. conceived and designed the research with input from R.d.E.; M.L. performed the experiments and analysis with assistance from R.d.E.; M.L. and H.D.M. wrote the paper, and all authors contributed to the development of the final manuscript.

Additional information

Supplementary information is available in the online version of the paper. Reprints and permissions information is available online at www.nature.com/reprints. Correspondence and requests for materials should be addressed to M.L. or H.D.M.

Competing financial interests

The authors declare no competing financial interests.

Methods

Data and pre-processing. In this study, we used the 1pctCO2 simulations from twelve CMIP5 Earth system models included in the CMIP5 model archive. This ensemble includes only the Earth system models (which include a dynamic carbon cycle) that participated in the CMIP5 1pctCO2 experiment[3]. In each of these runs, the atmospheric CO_2 concentration was increased at a rate of 1% per year from pre-industrial levels and simulations were integrated for 140 years up to a quadrupling of the initial CO_2 concentration. The models included in the current ensemble are BNU-ESM, CanESM2, CESM1-BGC, HadGEM2-ES, INMCM4, IPSL-CM5A-LR, IPSL-CM5A-MR, IPSL-CM5B-LR, MIROC-ESM, MPI-ESM-LR, MPI-ESM-MR and NorESM1-ME. For each of these models, only a single realization is available in the 1pctCO2 experiment. This ensemble is very similar to that used by Gillett *et al.*[3], although we did not include three of the 15 models used in their analysis. The CO_2 levels used for the two GFDL-ESM model versions (2G and 2M) were stabilized at $2\times CO_2$ rather than continuing until $4\times CO_2$, which did not allow the calculation of a 20-year average temperature change centred on year 70. We also excluded BCC-CSM1-1 because one variable (NBP) needed to diagnose the cumulative CO_2 emissions was not available from the ESGF website. For the analysis presented here, we interpolated all model results onto a common grid for analysis purposes (the CanESM2 grid with a resolution of 2.8°).

From global to regional TCRE. By definition[4], the TCRE is the change in surface air temperature per cumulative CO_2 emissions. Here, we define $\Delta T(m,\mathbf{x},t)$ as the temperature change simulated by the mth model in the ensemble, for the spatial domain $\mathbf{x}$, and calculated over time t. We can then write the global TCRE as:

$$\mathrm{TCRE}(m,t)=\frac{\langle \Delta T(m,\mathbf{x},t)\rangle}{E(m,t)} \tag{1}$$

where the E is the diagnosed value of the model's cumulative CO_2 emissions (calculated as the sum of the annual changes in the atmospheric CO_2 concentration and the CO_2 uptake by ocean and land carbon sinks), and $\langle . \rangle$ denotes the global spatial average. Similarly, the local to global ratio of temperature change (LGRTC), also known as 'simple pattern scaling'[6], can be written as:

$$\mathrm{LGRTC}(m,\mathbf{x},t)=\frac{\Delta T(m,\mathbf{x},t)}{\langle \Delta T(m,\mathbf{x},t)\rangle} \tag{2}$$

Because TCRE and LGRTC have both been shown to be relatively constant in time and across emission scenarios, their product should also be characterized by a similar such constancy. We thus define the regional TCRE (RTCRE) as:

$$\mathrm{RTCRE}(m,\mathbf{x},t)=\mathrm{TCRE}(m,t)\times\mathrm{LGRTC}(m,\mathbf{x},t)=\frac{\Delta T(m,\mathbf{x},t)}{E(m,t)} \tag{3}$$

We calculated all values as the difference between two 20-year average windows lagged by 70 years. This approach is consistent with previous studies[1,3] that recommended a standard calculation of the TCRE at the time when the atmospheric CO_2 has doubled its initial concentration in a scenario with a 1% CO_2 increase per year. We applied these calculations to the spatial temperature fields from each CMIP5 model, and then calculated the ensemble statistics for the range of twelve models included in the ensemble. We took the ensemble mean as the best estimate of the regional TCRE values, and represented the uncertainty range using one standard deviation of the models' responses.

Analysis of RTCRE uncertainty. The RTCRE pattern (equation (3)) is affected by two sources of uncertainty: natural climate variability and structural differences between models. The ensemble inter-model spread (IMS) of the TCRE pattern (σ^2_{IMS}) can thus be written as a sum of variances:

$$\sigma^2_{\mathrm{IMS}}=\sigma^2_{\mathrm{mod}}+\overline{\sigma^2_{\mathrm{IV}}} \tag{4}$$

where σ^2_{mod} is the model-uncertainty component of the inter-model spread and $\overline{\sigma^2_{\mathrm{IV}}}$ the ensemble mean (denoted by $\overline{(.)}$) internal variability (IV).

The availability of a only single realization per model in the 1pctCO2 experiment complicates the calculation of the internal variability component. To estimate the internal variability, we therefore began by calculating the natural climate variability (σ^2_1) of the detrended annual time series (using a fourth-order polynomial fit, as done in Hawkins *et al.*[21]). We then 'scaled' this variance for 20-year average time periods (σ^2_{20}) using the law of standard error:

$$\sigma^2_{20}=\frac{\sigma^2_1}{N}\frac{1+\phi}{1-\phi} \tag{5}$$

where N represents the number of years for an averaging period and $(1+\phi)/(1-\phi)$ is a variance inflation factor that accounts for the effect of lag-1 temporal autocorrelation (ϕ). Each term in (5) depends implicitly on the spatial coordinates and the model (m). Assuming that the internal variability of diagnosed global emissions is sufficiently small to be neglected, the internal variability affecting the TCRE pattern over a N-year period and for a given model can be written as:

$$\sigma^2_{\mathrm{IV}}=\frac{2\sigma^2_1}{NE^2}\frac{1+\phi}{1-\phi}$$

where $2\sigma^2_1$ represents the temperature change variance, and E^2 allows us to convert the temperature variability into the units of temperature change per CO_2 emission.

Contribution of pattern scaling versus global TCRE uncertainty. The inter-model spread of the RTCRE pattern (σ^2_{IMS}) can also be decomposed into the following variance components: uncertainty arising from variation in the global TCRE among models and the pattern of warming for a given global TCRE value. This can be done by writing the spatial pattern of temperature responses for the mth model as: $X_m(\mathbf{x})=G_m+P_m(\mathbf{x})$, where G_m is the global response and $P_m(\mathbf{x})$ the pattern deviation response around G_m. The sum of variances is therefore:

$$\sigma^2_{\mathrm{IMS}}=\sigma^2_{\mathrm{global}}+\sigma^2_{\mathrm{pattern}} \tag{6}$$

where $\sigma^2_{\mathrm{global}}$ is the variance of the global TCRE and $\sigma^2_{\mathrm{pattern}}$ is the variance contribution from the pattern of temperature changes only. The contribution of pattern deviations to the IMS can be written as the following ratio:

$$\sqrt{\frac{\sigma^2_{\mathrm{pattern}}}{\sigma^2_{\mathrm{IMS}}}} \tag{7}$$

Quantifying deviations from linearity. To characterize the relative linearity of global and regional temperature responses to cumulative CO_2 emissions, we used a commonly used measure to quantify the error of a fit: the sum of squared errors (SSE). Given a time series of temperature change (ΔT_i, for $i=1\ldots N$), a linear fit $\Delta\hat{T}=aE+b$ (where E is the value of cumulative emissions and a and b are the estimated regression coefficients) has an associated SSE defined as:

$$\mathrm{SSE}_{\mathrm{linear}}=\sum_i^N(\Delta T_i-\Delta\hat{T}(E_i))^2 \tag{8}$$

Similarly, this equation can be generalized to estimate SSE for a higher-degree polynomial fit. The ratio (Q) between the ensemble mean SSE for linear and quadratic fits ($\overline{\mathrm{SSE}}_{\mathrm{linear}}/\overline{\mathrm{SSE}}_{\mathrm{quadratic}}$) thus represents the quality of the linear versus quadratic fit, and can be written also in terms of the coefficient of determination R^2 as:

$$Q=\frac{\overline{\mathrm{SSE}}_{\mathrm{linear}}}{\overline{\mathrm{SSE}}_{\mathrm{quadratic}}}=\frac{1-\overline{R^2}_{\mathrm{linear}}}{1-\overline{R^2}_{\mathrm{quadratic}}} \tag{9}$$

We interpret Q as the ratio of 'unexplained variability' by the linear regression compared to a higher-degree (quadratic) polynomial. Q therefore represents the relative quadraticity of a time series. However, the signal-to-noise ratio (S) is also an important aspect to consider to better discriminate the degree of deviation from linearity, given that the ability to detect deviations from linearity (using calculated Q values) increases with decreasing variability in the time series. We thus define S as

$$S=\frac{\overline{\Delta T}}{\sqrt{\overline{\sigma^2_1}}} \tag{10}$$

where $\overline{\Delta T}$ is evaluated at the time of CO_2 doubling. The combination of Q and S values can therefore be used to assess the strength of the global TCRE deviation from linearity, which is evident from the overall pattern of higher Q values in areas with less variability (higher S values), and identify regions of stronger deviation from linearity, which are characterized by high Q values that can be detected despite relatively high variability (low S values).

References

21. Hawkins, E. & Sutton, R. The potential to narrow uncertainty in regional climate predictions. *Bull. Am. Meteorol. Soc.* **90,** 1095–1107 (2009).